

¹R. UMUNAKWE, ²O.C. OKOYE, ³U.S. NWIGWE,
⁴A. OYETUNJI, ⁵I.J. UMUNAKWE

EFFECTS OF STIRRING TIME AND PARTICLES PREHEATING ON POROSITY, MECHANICAL PROPERTIES AND MICROSTRUCTURE OF PERIWINKLE SHELL-ALUMINIUM METAL MATRIX COMPOSITE (PPS-ALMMC)

¹Department of Materials & Metallurgical Engineering, Federal University Oye-Ekiti, Ekiti State, NIGERIA

²Department of Mechanical Engineering, Federal University Oye-Ekiti, Ekiti State, NIGERIA

³Department of Mechanical & Mechatronics Engineering, Federal University Ndufu-Alike Ikwo, Ebonyi State, NIGERIA

⁴Department of Metallurgical & Materials Engineering, Federal University of Technology, Akure, NIGERIA

⁵Department of Chemistry, Federal University of Technology, Owerri, NIGERIA

Abstract: The effects of some process parameters on the properties of PPS-ALMMCs were investigated. Periwinkle shells were milled to 75 μ m particle size and the density of the particles determined. The particulate periwinkle shells (PPS) were used to reinforce aluminium 6063 alloy at 10wt% filler loading using two-step stir casting technique. Each specimen was stirred for five minutes in a semi-solid state before reheating to temperature above the liquidus, varying the stirring time for 3, 6 and 9 minutes respectively and casting in a metal die. A specimen was also produced with pre-heated filler. The effects of variation in stirring time and reinforcement pre-heating on the porosity, microstructure and mechanical properties of the composites were investigated. The results of the analysis show the composites possess lower density than the alloy and the addition PPS to aluminium alloy improves the strength, ductility and toughness over those of the alloy. The stirring time affects the way the PPS disperse in the matrix, the composites chemical homogeneity and mechanical properties. The best combination of chemical homogeneity, lowest porosity, and optimal improvement in strength, ductility, toughness was achieved when the composite materials was stirred for six minute above the liquidus temperature compared to the other specimens.

Keywords: Composites, mechanical properties, periwinkle shells, porosity, stirring time

1. INTRODUCTION

Due to their specific strength, stiffness, hardness and wear resistance, aluminum metal matrix composites (ALMMCs) are considered attractive materials for various engineering applications especially for weight sensitive applications over conventional copper tungsten (CuW) and copper molybdenum alloys (Babalola, et.al., 2015); (Yawas, et.al., 2016). Although, particulate crystalline ceramic materials such as SiC, Al₂O₃, TiC, TiC, etc. have been used to reinforce aluminium alloys in order to improve the mechanical, wear, thermal and other properties of the composites over the alloy, the composite materials are however more expensive and heavier than the alloy (Gladston, et.al., 2015).

The use of agricultural wastes as fillers for composite materials presents opportunities to reduce the cost of composite materials. Agricultural wastes are cheap, readily available, and renewable and add to solid wastes. Researchers have reported the use of agricultural wastes such as rice husks to improve the properties of AA6061 alloy (Gladston, et.al., 2015); particulate coconut shell to reinforce recycled aluminium can (Agunsoye, et.al., 2104); and rice husk ash (RHA) as the reinforcement for aluminium (AlSi10Mg)-RHA composites (Saravanan and Senthilkumar, 2014). It was reported that these





agricultural wastes provided useful reinforcements in aluminum matrices at lower particle sizes as well as distribute uniformly. Researchers investigated and reported the use of particulate periwinkle shell as reinforcement for cashew nut shell liquid (Ofem and Umar, 2012); (Ofem, et.al., 2012); polyester resin (Njoku, et.al., 2011); (Onyechi, et.al., 2015); and phenolic resin (Yakubu, et.al., 2013); (Yawas, et.al., 2016).

Particulate periwinkle shell reinforced composites exhibited higher tensile strength, compressive strength, wear resistance and also lower density than the unreinforced matrices. It is interesting to know that particulate periwinkle shell refines the grains of aluminium alloy and improves mechanical properties in smaller particle sizes (Umunakwe, et.al., 2017). The properties of the composite materials are affected by factors such as the type of reinforcement, the method of production, the method of stirring, the volume or mass fraction of reinforcement, the particle size of the reinforcement, the shape and distribution of the reinforcement in the matrix (Mark, et.al., 1999); (Kuma, et.al., 2010). In this work, we investigated the effects of stirring time and particle preheating on the mechanical properties and microstructure of PPS-ALMMCs.

2. MATERIALS AND METHOD

≡ Materials:

The major materials are aluminium 6063 (AA6063) ingot procured from NIGALEX, Lagos, Nigeria and while periwinkle shells sourced from a local market in Otueke, Bayelsa State, Nigeria. The composition of the ingot is shown in Table 1. The preparation of the periwinkle shells involves washing with tap water, boiling in water at 100°C for 45 minutes and rewashing to remove all dirt, sands and any form of contamination, followed by sun drying for three days. They were then placed in an oven and heated to 120°C for 45 minutes so as to remove all moisture. The shells were then crushed with a hammer mill to reduce the particles sizes and then transferred to ball mill where they were grinded. Milled periwinkle shells were sieved with standard sieves to obtain the required 75µm particulate periwinkle shells (PPS). The PPS was used as the filler for composites fabrication.

Table 1: Composition of the Aluminium Ingot

Element	Al	Si	Fe	Cu	Mn	Mg	Zn	Cr
Average content	98.19	0.5953	0.4635	0.0117	0.0244	0.3359	<0.002	0.0107
Element	Ni	Ti	Sr	Zr	V	Ca	Be	
Average content	0.0347	0.0566	<0.000	0.0772	0.0114	>0.070	<0.000	

≡ Chemical Analysis of PPS:

The elemental composition of the PPS was determined using X-ray Fluorescence Spectrometer which detects elements between sodium (Na, Z=11) and uranium (U, Z =92). The major element present in PPS is calcium as shown in Table 2.

Table 2: Elemental Composition of PPS

Element	Ca	Fe	Si	Mo	Al	P	S	Sn	Sb	Other elements
Content	70.3350	0.5066	0.0724	0.2372	0.1938	0.2746	0.3987	0.4561	0.4511	27.0745

≡ Production of the PPS-ALMMCs:

The production of the composite materials followed the method described by (Alaneme and Bodunrin, 2013). The required quantities of AA6063 alloy and PPS for the production PPS-ALMMCs with 10wt% reinforcement were calculated based on percentage of the total weight and measured using a digital electric balance (Model XYC 3000, sensitivity 0.01g).

The aluminium ingot was charged into a gas-fired crucible furnace and heated to 730°C ± 30°C for melting. The melted AA6063 alloy was allowed to cool in a furnace to about 600°C and it changed to a semi-solid state. The weighed PPS was added to the semi-solid melt and the mixture was stirred manually for five minutes with a stainless steel spindle. The composite slurry was then re-heated to 730°C. At this temperature, the composite was stirred vigorously and the stirring times were varied for various specimens in order to measure the effects of variation of stirring time.

For the production of specimen 3, the required quantity of PPS was preheated to 300°C for five minutes and then added to melt in semi-solid state and the composite material produced following the same procedure. Table 3 shows various specimens of the composite materials produced with their stirring times. The specimens were cast in a metallic die. Control sample was cast without the addition of the PPS.





Table 3: Various Specimens of PPS-ALMMCS Produced.

Specimen	Weight percent of PPs (wt%)	Preheating of PPS	Stirring time in semi-solid state (minutes)	Stirring time in liquid state after re-heating (minutes)
1	00 (control)	No	5	3
2	10	No	5	0 (Not stirred)
3	10	Yes	5	3
4	10	No	5	3
5	10	No	5	6
6	10	No	5	9

≡ **Determination of the Density of the PPS:**

The density of PPS was determined using distilled water, density bottle and digital electric balance (Model XYZ 3000, sensitivity 0.01g). Empty density bottle was weighed and the weight was recorded as M_0 . The empty density bottle was filled with water and weighed (M_1) and the mass of water that fills it, M_{w1} , calculated from equation (1).

$$M_{w1} = M_1 - M_0 \quad (1)$$

The volume of water that fills it was calculated from equation (2), where p_w is the density of water ($1g/cm^3$)

$$V_{w1} = \frac{m_w}{p_w} \quad (2)$$

The density bottle was emptied and dried. A quantity of $75\mu m$ PPS was added to the empty density bottle and the weight of the density bottle together with the PPS measured as M_2 . The weight of the PPS, M_{pps} , added was calculated from equation (3).

$$M_{pps} = M_2 - M_0 \quad (3)$$

Water was added to fill the bottle and the weight of the whole content, M_c , taken to determine the weight of water added as M_{w2} ;

$$M_{w2} = M_c - M_2 \quad (4)$$

The volume of water (V_{w2}) added was determined from equation (5)

$$V_{w2} = \frac{m_{w2}}{p_w} \quad (5)$$

The volume of the PPS (V_{pps}) put in the density bottle was calculated from equation (6)

$$V_{pps} = V_{w1} - V_{w2} \quad (6)$$

$$\text{Density of PPS} = \frac{M_{pps}}{V_{pps}} \quad (7)$$

≡ **Determination of Densities and Porosities of Alloy and Composite Materials:**

The basic method of calculating density is by dividing mass by volume. In this work, experimental density of each specimen was determined by Archimedes' principle. The theoretical densities of the composites were calculated from the rule of mixture as shown in equation (8). The weight percentage of PPS in the composites was converted to volume fractions using the density of PPS calculated in equation (7) and the density of the alloy in order to convert the mass of the alloy and PPS to their volumes so as to accurately calculate the theoretical density.

The difference between the theoretical and experimental density of each composite specimen was used to estimate porosity using equation (9) (Hizombor, et.al., 2010).

$$p(\text{PPS-ALMMC}) = p(\text{AA6063}) \times V_f(\text{AA6063}) + p(\text{PPS}) \times V_f(\text{PPS}) \quad (8)$$

where: $p(\text{PPS-ALMMC})$ = Theoretical density of composites, $p(\text{AA6063})$ = Density of AA6063 alloy, $V_f(\text{AA6063})$ = Volume fraction of AA6063 alloy, $p(\text{PPS})$ = Density of PPS and $V_f(\text{PPS})$ = Volume fraction of PPS.

$$\text{Porosity} = \frac{\text{Theoretical density} - \text{Experimental density}}{\text{Theoretical density}} \quad (9)$$





≡ **Tensile Testing:**

Each specimen was machined for tensile testing and Instron Universal Testing Machine (UTM) was used to run the tensile tests on the machined samples at room temperature and strain rate of 10mm/s in accordance with ASTM standard (ASTM E8M, 1991). The gauge length and gauge diameter for each specimen was 29 mm and 4.5 mm respectively. The parameters were imputed in the UTM software and the tests were run to obtain the tensile properties. Three repeated tests were carried out on each specimen to guarantee reliability.

≡ **Hardness Testing:**

A Digital Brinell Hardness Testing Machine with 10mm indenter and applied load of 125Kgf was used to measure the hardness of each specimen. The length and diameter of each specimen for hardness testing were 25x25mm respectively. The dwell time for each hardness test was 30s. Three hardness tests were carried out on each specimen and the average value reported as the hardness of the specimen. The hardness values recorded as Brinell Hardness Number (BHN) were obtained digitally from the image analysis of the computer attached to the machine.

≡ **Microstructural Analysis:**

Energy Dispersive X-ray Scanning Electron Microscope (Phenom SEM with EDX) was used to study the surface morphology of all composite at magnification 542 and the EDX analysis was done at different spots in the micrograph for each specimen in order to do elemental compositional analysis from the EDX spectrum of the various spots on a specimen so as to ascertain chemical homogeneity of the composites.

3. RESULTS AND DISCUSSIONS

≡ **Density and Porosity:**

The particle density of PPS determined was 1.3g/cm³ while the density of the AA6063 alloy was 2.5g/cm³. Since PPS has lower density than aluminum 6063 alloy, its addition to the alloy to produce composite will make the density of the composite to be less than that of the alloy. At the same volume, PPS-ALMMCs will weigh less than aluminium alloy. At 10wt% filler loading, the theoretical density of the composite material estimated from the rule of mixture was 2.2845 g/cm³. This is a positive development because it will further maximize the utilization of PPS-ALMMC where lighter weight is desired and properties such as specific strength and stiffness will be higher in the composite compared to the aluminium alloy.

Table 4: Density of AA6063 Alloy; Densities and Percentage Porosities of PPS-ALMMC with 75µm Particulate PPS at 10wt Filler Loading

Specimen	Theoretical density (g/cm ³)	Experimental density (g/cm ³)	Porosity (%)
1 (alloy)	-	2.5	-
2	2.284	2.05	2.70
3	2.284	2.26	1.05
4	2.284	2.21	3.24
5	2.284	2.28	0.002
6	2.284	2.28	0.002

The densities and porosities of the various specimens are shown in Table 4. Porosity or void in the composite material accounts for the difference between the theoretical and experimental densities of the composite materials. Porosity is as a result of trapped air or poor wettability of the reinforcement. High porosity results to low strength and other mechanical properties.

Two-step casting has been reported as a method used to reduce porosity during stir casting and the acceptable percentage of porosity in a composite material is within range of less than 5% (Alaneme and Bodunrin, 2013). From the results shown in Table 4, the porosity of all the specimen were within the acceptable levels of less than 5% despite the stirring time above the liquidus temperature after the initial stirring in a semi solid state. However, stirring for a longer time reduced the porosity to a very insignificant value.

≡ **Microstructure**

The SEM micrograph of the alloy is shown in Figure 1 while those of the composites are shown in Figures 2 to 6. The elemental composition gotten from the EDX spectrum of each labeled spot in the micrograph of each specimen is shown in Table 5.

The percentage of oxygen at the near the surface of the cast alloy showed that air was trapped at the surface during solidification while the core lacked oxygen and has over 98% aluminum with traces of other elements. The surface of the alloy was machined out during all the tests in order to ensure





accuracy of the results. The stirring time above the liquidus temperature and reinforcement preheating affected the distribution of the PPS in the matrix.

Table 5: Elemental composition of the various spots labeled in the micrographs obtained from EDX analysis

Specimen	Elemental composition of various spots in the microstructure					
	Spots					
	1	2	3	4	5	6
1	Al(88.5%), O(11.3%), Ca(0.2%).	Al(99.8%), Ca(0.2%).	Br(99.8%), Ca(0.2%).	-	-	-
2	Al(93%), O(6.7%), Ca(0.3%).	Al(99.7%), Ca(0.3%).	Al(82.9%), C(8.3%), Cl(1.7%), O(6.5%), Ca(0.5%).	Al(82.0), C(17.4), Ca(0.6).	Al(99.7), Ca(0.3%).	Al(94.1%), O(5.6%), Ca(0.3%).
3	Al(99.7%), Ca(0.3%).	Al(99.8%), Ca(0.2%)	Al(99.8%), Ca(0.2%).	Al(100%).	Al(98.0%), As(1.8%), Ca(0.2%)	Al(99.9%), Ca(0.1%)
4	Al(32.6%), O(15.4%), Ca(0.2%).	Al(91.0%), O(8.8%), Ca(0.2%).	Al(60.9%), C(27.7%), O(11.2%), Ca(0.2%)	Al(32.6%), O(51.8%), K(4.2%), Na(6.9%), Cl(3.1%), Ca(1.4%).	Br(99.2%), Ca(0.8%).	Al(99.5%), Ca(0.5%).
5	Al(100%).	Al(98.4%), Ca(1.6%).	Al(99.6%), Ca(0.4%).	Al(99.8), Ca(0.2%).	Al(99.8%), Ca(0.2%).	Al(99.7%), Ca(0.3%).
6	Al(99.9%), Ca(0.1%)	Al(99.4%), Ca(0.6%).	Al(98.5%), As(1.5%).	Al(100%).	Al(100%).	Al(99.5%), Ca(0.5%).

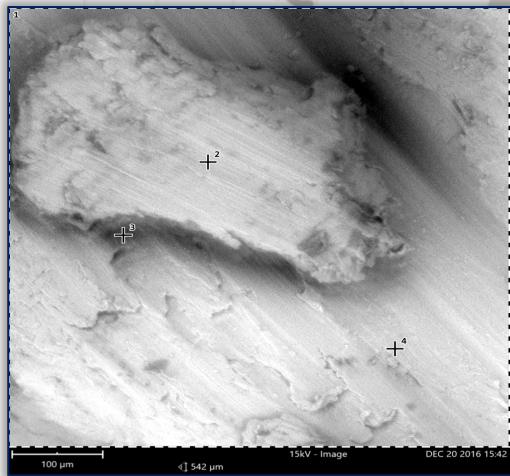


Figure 1: Micrograph of AA6063 alloy (Specimen 1)

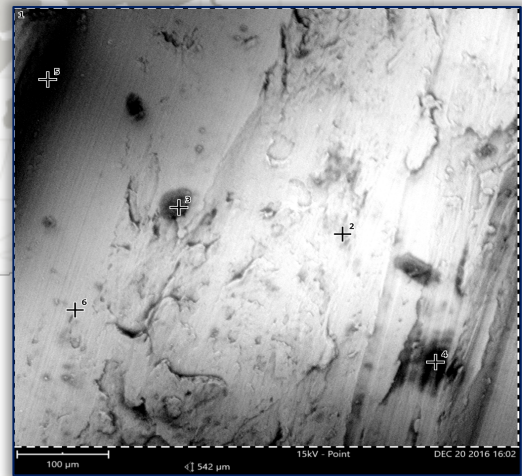


Figure 2: Micrograph of PPS-ALMMC (specimen 2)

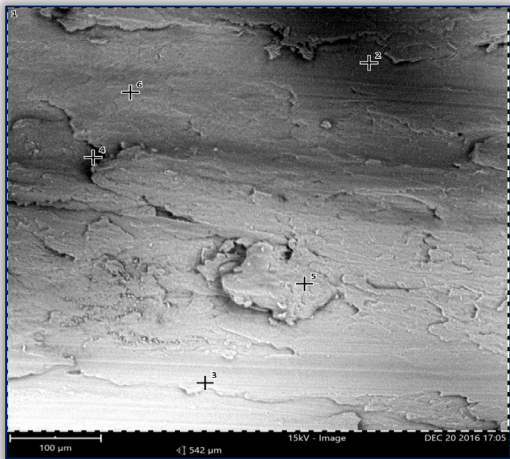


Figure 3: Micrograph of PPS-ALMMC (specimen 3)

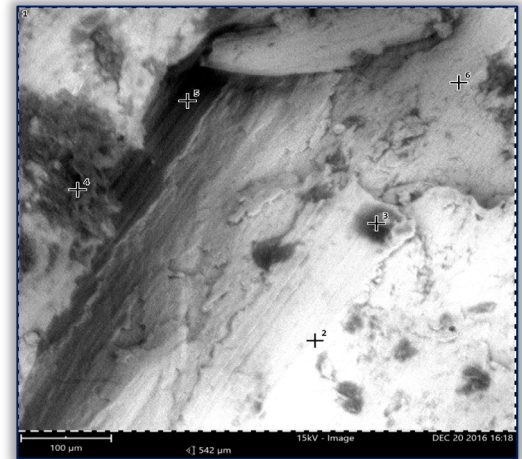


Figure 4: Micrograph of PPS-ALMMC (specimen 4)



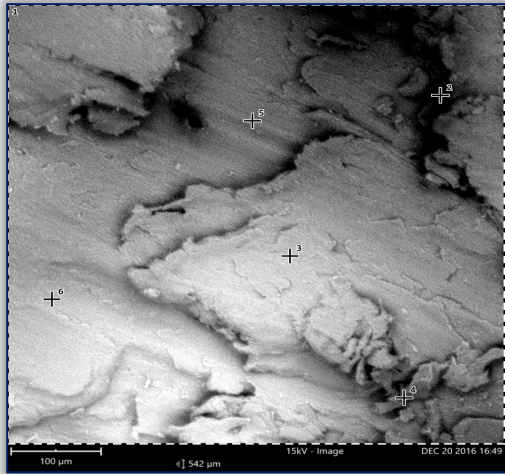


Figure 5: Micrograph of PPS-ALMMC (specimen 5)

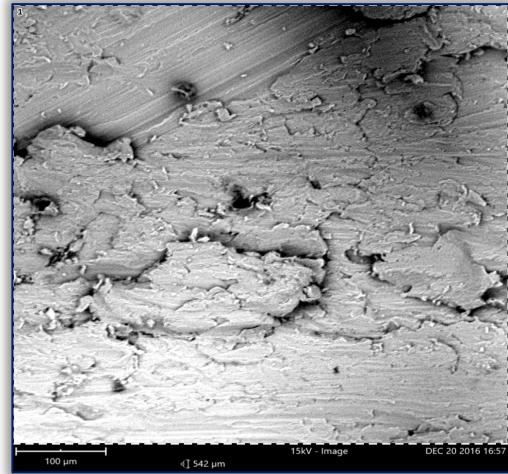


Figure 6: Micrograph of PPS-ALMMC (specimen 6)

The micrograph shown in Figure 2 showed that no stirring above the liquidus temperature made the PPS to agglomerate and formed spheroids (those black spherical shapes) which were distributed in the matrix as the EDX analysis of the spheroid showed elements from PPS. The presence of the spheroids in the matrix which impeded dislocation movements improved the mechanical properties of the composite despite the oxygen trapped near the surface as a result of no stirring. Specimen 4 with the micrograph shown in Figure 4 also showed PPS spheroids in the matrix with higher porosity since the stirring time of three minutes was not enough to break the spheroids and distribute PPS. Specimens 2 (not stirred above the liquidus) and 4 (stirred for 3 minutes above the liquidus) lack chemical homogeneity and this may result in the variation of properties in the composites when cast in large size. The micrograph of specimen 5 is shown in Figures 5. With the stirring time of about six minutes, the composite produced showed chemical homogeneity and least porosity, the PPS are more evenly distributed and finer in the matrix. Figure 6 shows the micrograph of specimen 6 stirred for nine minutes above the liquidus temperature. As observed in Figure 6, the PPS agglomerated in longer distance leaving the major part of the matrix without reinforcement. Also, specimen 3 which was produced with preheated PPS showed even distribution of the PPS in the matrix.

≡ Mechanical Properties

The introduction of PPS in AA6063 alloy at small particle size has been reported to increase the strength, ductility and toughness because of the ability of PPS to refine the grains of the matrix (Umunakwe, et.al., 2017); (Njoku, et.al., 2011); (Ofem and Umar, 2012). The result of this work follows the same trend. However, the stirring time above the liquidus temperature and PPS preheating affect the degree of improvement observed in the composites.

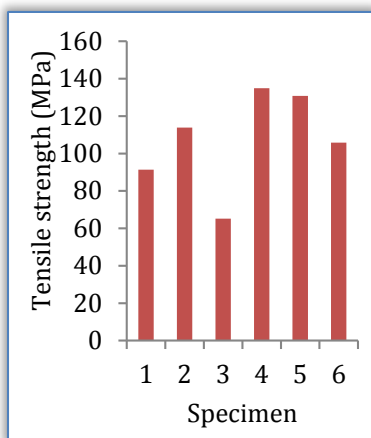


Figure 7: Tensile strengths of AA6063 alloy and Al-PPS composites

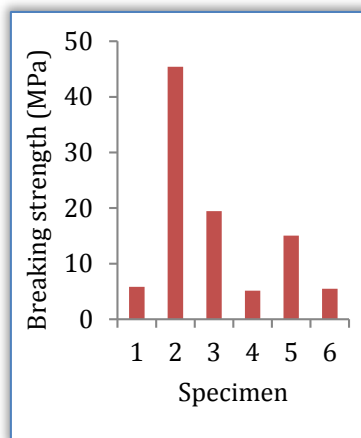


Figure 8: Breaking strengths of AA6063 alloy and Al-PPS composites

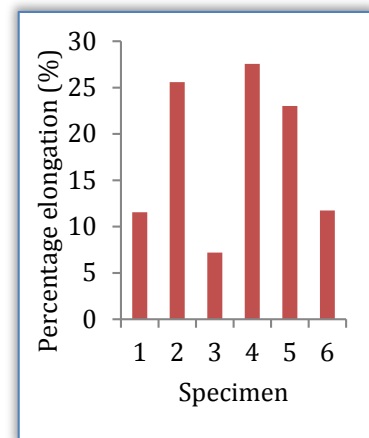


Figure 9: Percentage elongations of AA6063 alloy and Al-PPS composites



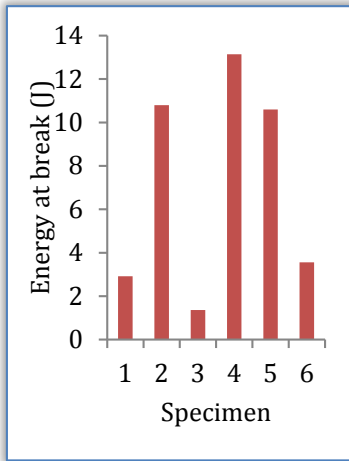


Figure 10: Energies at break of AA6063 alloy and Al-PPS composites

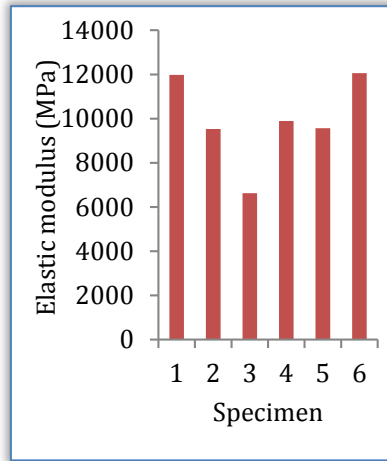


Figure 11: Elastic moduli of AA6063 alloy and Al-PPS composites

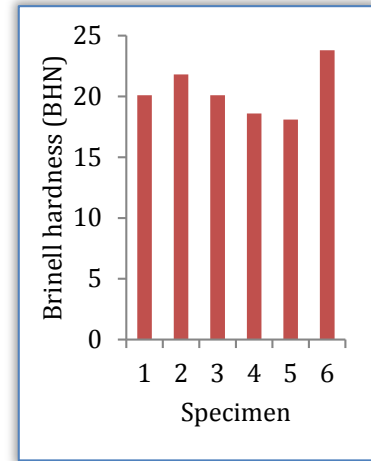


Figure 12: Brinell hardness of AA6063 alloy and Al-PPS composites

Figures 7-10 and Figure 12 show improved tensile, breaking strength, ductility, toughness and hardness of specimen 2 which was not stirred above the liquidus. The improved properties are as a result combined ability of PPS to refine the grains and PPS spheroids formed in the matrix. Specimen 4 shows the same trend but presented a lower breaking strength than the alloy higher porosity and chemical heterogeneity.

Specimen 5 showed the best combination of improvement in strength, ductility and toughness as shown in Figures 7-10. The particles are distributed more finely in the micrograph shown in Figure 5 and chemical homogeneity was observed as shown in Table 5 when the composite was stirred for six minutes above the liquidus and hence the improvement in strength, toughness and ductility.

Specimen 6 did not show significant improvement in strength, toughness and ductility because the major part of the composite lack the grain refining PPS after long stirring time. Preheating of PPS before its addition to AA6063 alloy produced composite with reduced tensile strength, toughness and ductility because the chemistry of the PPS was altered during preheating and the preheated PPS lacks the reinforcing ability of the unheated PPS.

The elastic moduli and hardness of composites shown in Figures 11 and 12 also follow the trend earlier reported (Umunakwe, et.al., 2017). Improvement in hardness and elastic modulus can be achieved at higher weight fraction of the 75 μ m PPS in the matrix as earlier reported (Umunakwe, et.al., 2017). Specimen 6 showed higher hardness and slight improvement in elastic modulus because of the low toughness exhibited by the composite as shown in Figures 9-12.

CONCLUSIONS

From the results of this work, the following can be concluded;

- ≡ PPS preheating and the stirring time above the liquidus temperature of PPS-ALMMCs affect the distributions of PPS in the matrix and the properties.
- ≡ The optimal stirring time above the liquidus is six minutes in order to get a combination of improved mechanical properties.
- ≡ Preheating PPS prior to its use as filler in aluminium alloy does not improve the mechanical properties.
- ≡ The lighter weight, higher strength, toughness, ductility, specific strength, stiffness and hardness of PPS-ALMMC composites makes is attractive for applications such as in car cylinder liners, aluminum calipers and other diverse applications where weight, strength and toughness are major concern.

References

- [1.] Agunsoye, J., Talabi, S., Bello, S., & Awe, I. (2104). The Effects of Cocos Nucifera (Coconut Shell) on the Mechanical and Tribological Properties of Recycled Waste Aluminium Can Composites. *Tribology in Industry*, 36(2), 155-162.
- [2.] Alaneme, K., & Bodunrin, M. (2013). Mechanical Behaviour of Alumina Reinforced AA6063 metal matrix composites developed by two-step casting process. *ACTA TECHNICA CORVINIENSIS-Bulletin of Engineering*, 6(3), 105-110.





- [3.] ASTM E8M. (1991). Standard Test Method for Tension of Metallic Materials (Metric) in Annual Book of ASTM Standards. Philadelphia: American Society of Testing and Materials.
- [4.] Babalola, P., Inegbenegbor, A., Bolu, C., & Inegbenegbor, A. (2015). The Development of Molecular-Based Materials for Electrical and Electronic Applications. The Journal of The Minerals, Metals & Materials Society, 67(4), 830-833. doi:DOI 10.1007/s11837-015-1355-2
- [5.] Gladston, J. A., Sheriff, N. M., Dinaharan, I., & Selvam, J. D. (2015). Production and characterization of rich husk ash particulate reinforced AA6061 aluminum alloy composites by compocasting. Transaction of the Nonferrous Society of China, 25, 683-691.
- [6.] Hizombor, M., Mirbagheri, S., & Abdideh, R. (2010). Casting of A356/TiB Composite based on the TiB₂p/CMC/PPS mortar. Metal 2010. Czech Republic: Roznov pod Radhostem.
- [7.] Kuma, G. B., Rao, C. S., Selvaraj, N., & Bhagyashekar, M. S. (2010). Studies on Al6061-SiC and Al7075-Al₂O₃ Metal Matrix Composites. Journal of Minerals & Materials Characterization & Engineering, 9(1), 43-55.
- [8.] Mark, O. M., Adams, R., Fennessy, K., & Hay, R. A. (1999). Aluminum Silicon Carbide (AlSiC) for Advanced Microelectronic Packages. Ceramics Process Systems Corp, IMAPS May 1998 Boston Meeting, 1-6.
- [9.] Njoku, R., Okona, A., & Ikpaki, T. (2011). Effects of variation of particle size and weight fraction on the tensile strength and modulus of periwinkle shell reinforced polyester composite. Nigerian journal of technology, 30(2), 87-93.
- [10.] Ofem, M. I., & Umar, M. (2012). Effect of filler content on the mechanical properties of periwinkle shell reinforced CNSL resin composites. ARPN Journal of Engineering and Applied Sciences, 7(2), 212-215.
- [11.] Ofem, M. I., Abam, F. I., & Ugot, I. U. (2012). Mechanical properties of hybrid periwinkle and rice husk filled CNSL composite. International Journal of Nano and Material Sciences, 1(2), 74-80.
- [12.] Onyechi, P. C., Asiegbu, K. O., Igwegbe, C. A., & Nwosu, M. C. (2015). Effect of volume fraction on the mechanical properties of periwinkle shell reinforced polyester composite (PRPC). American Journal of Mechanical Engineering and Automation, 2(1), 1-15.
- [13.] Saravanan, S., & Senthilkumar, M. (2014). Mechanical Behavior of Aluminum (AlSi10Mg)-RHA Composite. International Journal of Engineering and Technology, 5(6), 4834-4840.
- [14.] Umunakwe, R., Olaleye, D. J., Oyetunji, A., Okoye, O. C., & Umunakwe, I. J. (2017). Assessment of the mechanical properties of particulate periwinkle shell-aluminium 6063 metal matrix composites (PPS-ALMMC) produced by two-step casting. Nigerian Journal of Technology, 36(2), In press.
- [15.] Yakubu, A. S., Amaren, S., & Yawas, D. S. (2013). Evaluation of the wear and thermal properties of asbestos free brake pad using periwinkles shell particles. Usak University Journal of Material Sciences, 1, 1999-108.
- [16.] Yawas, D., Aku, S., & Amaren, S. (2016). Morphology and properties of periwinkle shell asbestos-free brake pad. Journal of King Saud University – Engineering Sciences, 28, 103-109

ANNALS of Faculty Engineering Hunedoara
– International Journal of Engineering



copyright © UNIVERSITY POLITEHNICA TIMISOARA,
FACULTY OF ENGINEERING HUNEDOARA,
5, REVOLUTIEI, 331128, HUNEDOARA, ROMANIA
<http://annals.fih.upt.ro>

